

AN EXACT SOLUTION OF MECHANICAL BUCKLING FOR FUNCTIONALLY GRADED MATERIAL BIMORPH CIRCULAR PLATES

Jafar Eskandari Jam*, Mahmood Khosravi,
Nader Namdaran

Composite Materials & Technology Center, Tehran, Iran

Received 25.06.2012

Accepted 20.07.2012

Abstract

Presented herein is the exact solution of mechanical buckling response of FGM (Functionally Graded Material) bimorph circular plates, performed under uniform radial compression, by means of the classic theory and the non-linear Von-Karman assumptions, for both simply supported and clamped boundary conditions. Material properties are assumed to be symmetric with respect to the middle surface and are graded in the thickness direction according to a simple power law, in a way that the middle surface is pure metal and the two sides are pure ceramic. Using the energy method the non-linear equilibrium equations are derived and the stability equations have been used, so as to determine the critical buckling pressure, considering the adjacent equilibrium criterion, and finally a closed-form solution has been achieved for it. The effect of different factors, including thickness to radius variation rate of the plate, volumetric percentage of material index, and Poisson's ratio on the critical buckling compression have been investigated for two simply supported and clamped boundary conditions, and the results achieved are compared with each other and the results available in the literature.

Keywords: Mechanical buckling analysis, circular plates, functionally graded materials, classic theory.

Introduction

In the recent years, functionally graded materials (FGMs) have been widely used in advanced industries especially in aerospace and nuclear engineering applications, and due to their importance they have always been attractive for designers, and many research studies have been performed on this topic. Generally, FGMs are not homogeneous and are composed of a mixture of ceramic and metal, or a mixture of

* Corresponding Author: Jafar Eskandari Jam, jejaam@gmail.com

different metals. Microscopically, FGMs are non-homogenous and their structural properties including distribution type and the size of the phases vary continuously and homogeneously across the thickness, and this variation results in the gradual change of mechanical properties for these materials [1].

Stability analysis and studies on the buckling behavior of plates have always been considered as one of the most important subjects in structural analysis. The first solution of the stability problem for plates was presented by Brayan [2] in 1891. In this study, the buckling of a circular plate under uniform radial loading was performed for the clamped boundary conditions.

Yamaki [3] investigated the buckling of annular plates under loadings applied on the inner and outer edges, and showed that buckling in this state does not necessarily happen in the first mode.

Timoshenko and Gere [4] studied the buckling analysis problem of different engineering structures including: columns, frames, curved beams, plates and shells.

After that Almorh and Brush [5] presented a general analysis of buckling for columns, plates, and shells, and also investigated different methods of formulation for the non-linear equilibrium and stability equations.

Reddy and Khdeir [6] studied the buckling analysis and free vibrations of composite laminated rectangular plates, using the classic, the first and the third order shear theories, under different boundary conditions. In addition to the analytical solution, numerical solution was done on the basis of the finite element method in this paper. Results of this study indicate that the classic theory overestimates the natural frequencies and critical buckling load, and as the thickness to lateral length ratio increases, this discrepancy increases.

Raju et al. [7, 8] investigated the post buckling of the homogenous and orthotropic circular plates with linear thickness variation, under mechanical and thermal loadings, in terms of the uniform temperature rise. Thermal buckling analysis of these plates was carried out, using finite element theory.

Ozakca et al. [9] using finite element method and taking into account the shear effects as the first order shear theory; performed the buckling analysis and thickness optimization for the circular and annular plates.

Najafizadeh and Eslami [10, 11] studied buckling analysis of the one-sided FGM circular plates, under different types of thermal loading, for the clamped boundary conditions, and also for radial mechanical compression loading, under simply supported and clamped boundary conditions. In these studies, the classic theory was used and the analytical solutions were provided. Najafizadeh and Hedayati [12] have performed the thermal and mechanical buckling analyses for one-sided FGM circular plates, using the first order shear theory and have compared the results achieved with the classic theory. In this study, thermal buckling analysis was performed only for the clamped boundary conditions, and the mechanical buckling analysis was performed for both the simply supported and clamped boundary conditions. Najafizadeh and Heydari [13, 14] have investigated the buckling analysis of one-sided FGM circular plates, under different thermal loadings, for the clamped boundary conditions, and also investigated it for uniform radial compression loading, under simply supported and clamped boundary conditions. In these studies, the third order shear theory has been used, and the results obtained are compared with the results of the classic and first order shear theories.

Naei et al. [15] studied the mechanical buckling of one-sided FGM circular plates with variable thickness, under uniform radial compression, using finite element technique. The boundary conditions used for the circular plate were simply supported and clamped. Jalali et al. [16] performed the thermal stability analysis for circular functionally graded sandwich plates of variable thickness and FGM face sheets, using pseudo-spectral method. In this study, the circular plate is under a uniform thermal loading, and is presented according to the first order shear theory.

FGM plates can be of two types, namely, one-sided FGMs and FGM bimorphs, based on their property variations across the thickness, as shown in figure 1. One-sided FGM plates have pure ceramic on one side and pure metal on the other side; and the material properties vary continuously from one side to the other. But in FGM bimorph plates, both sides are pure ceramic and the mid-plane is pure metal.

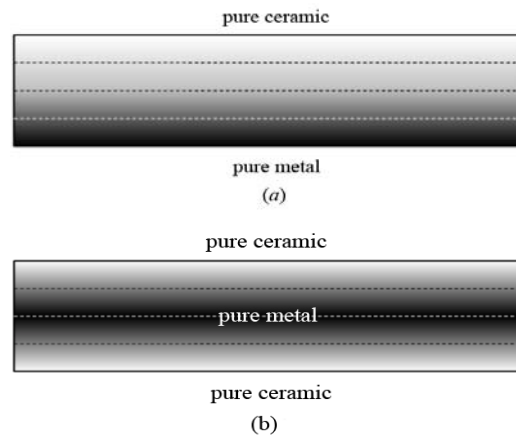


Figure 1 .FGM plate: (a) one-sided, (b) bimorph.

In this study, the classic theory and the Von Karman assumptions have been used to analyze the mechanical buckling of FGM bimorph circular plates, under uniform radial compression. In order to determine the non-linear equilibrium equations, the minimum potential energy has been used, and by application of the perturbation method, the non-linear equilibrium equations have become linear. In order to determine the critical buckling pressure, the stability equations have been derived, using the adjacent equilibrium criterion from the linear equilibrium equations, and then are analytically solved for simply supported and clamped boundary conditions, and a closed-form solution is provided for it, later on.

The effect of different factors, including thickness to radius variation rate of the plate, volumetric percentage of material index, and Poisson's ratio on the critical buckling pressure have been investigated for two simply supported and clamped boundary conditions, and the results achieved are compared with the results obtained for homogenous and one-sided FGMs.

Formulation of the problem

Properties of the FGM

The circular plate studied, is composed of FGM bimorph materials in which the volumetric percentage of ceramic and as a result the properties of the material are symmetric with respect to the middle surface, and vary continuously through the thickness direction, in a way that the middle surface is pure metal and as we approach the outer surfaces, the ceramic percentage increases and at the upper and lower surfaces, i.e. at $z = -\frac{h}{2}$ and $z = \frac{h}{2}$ it becomes pure ceramic.

Since FGMs are a compound of metal and ceramic, properties of these materials like the modulus of elasticity E , based on the classic linear rule of mixtures are expressed as follows:

$$E_f = E_m V_m + E_c V_c \quad (1)$$

Wherein c and m show the properties of the ceramic and metal, respectively, and V_c and V_m indicate their respective volume fractions [16].

Here, the variations of the material properties like the modulus of elasticity are expressed by the simple power law as follows [17]:

$$P^1(z) = P_m + (P_c - P_m) \left(-\frac{2z}{h}\right)^n, \quad -\frac{h}{2} \leq z \leq 0 \quad (2)$$

$$P^2(z) = P_m + (P_c - P_m) \left(\frac{2z}{h}\right)^n, \quad 0 \leq z \leq \frac{h}{2}$$

P shows the material properties and can be the modulus of elasticity. Variation of the Poisson's ratio is negligible and is supposed to be constant. n is the volume fraction index of the FGM, which indicates the compound of the volume fractions of the ceramic and metal across the thickness, which can be bigger than or equal to zero. The zero and infinity values for this index mean pure ceramic and pure metal, respectively.

Stability and equilibrium equations

A circular FGM bimorph plate with radius a and thickness h is considered. The displacement field according to the classic theory can be expressed in the polar coordinates with axisymmetry, as follows [19]:

$$U(r, z) = u(r) - z \frac{dw}{dr} \quad (3)$$

$$V = 0, \quad W(r, z) = w(r)$$

Where U , V , and W are displacements along r , θ , and z axes and $u(r)$, $w(r)$ are displacements of the middle surface along r and z directions.

The buckling problem is categorized in the non-linear geometrical problems, and in non-linear problems, displacements are in a range that the non-linear strain-displacement terms cannot be disregarded. The strain-displacement relations based on the Von-Karman assumptions, and relation (3) can be stated as [19]:

$$\varepsilon_r = \frac{dU}{dr} + \frac{1}{2} \left(\frac{dW}{dr} \right)^2, \quad \varepsilon_\theta = \frac{U}{r}, \quad \gamma_{r\theta} = 2\varepsilon_{r\theta} = 0 \quad (4)$$

$$\begin{Bmatrix} \varepsilon_r \\ \varepsilon_\theta \\ \gamma_{r\theta} \end{Bmatrix} = \begin{Bmatrix} \varepsilon_{r0} \\ \varepsilon_{\theta0} \\ \gamma_{r\theta0} \end{Bmatrix} + z \begin{Bmatrix} k_r \\ k_\theta \\ k_{r\theta} \end{Bmatrix} \quad (5)$$

And, the strains of the middle surface are given by:

$$\varepsilon_{r0} = \frac{du}{dr} + \frac{1}{2} \left(\frac{dw}{dr} \right)^2, \quad \varepsilon_{\theta0} = \frac{u}{r}, \quad \gamma_{r\theta0} = 0 \quad (6)$$

The curvatures are defined as:

$$k_r = - \left(\frac{d^2w}{dr^2} \right), \quad k_\theta = - \frac{1}{r} \left(\frac{dw}{dr} \right), \quad k_{r\theta} = 0 \quad (7)$$

Regarding the fact that the materials are isotropic, by disregarding the stresses in the thickness direction and taking the Poisson's ratio to be constant, the strain-displacement relations are achieved as follows [15]:

$$\begin{aligned} \sigma_r &= \frac{E}{1-\nu^2} (\varepsilon_r + \nu\varepsilon_\theta) \\ \sigma_\theta &= \frac{E}{1-\nu^2} (\varepsilon_\theta + \nu\varepsilon_r) \\ \tau_{r\theta} &= \frac{E}{2(1+\nu)} \gamma_{r\theta} = 0 \end{aligned} \quad (8)$$

In the above relations, E is the modulus of elasticity for the FGM. σ_θ and σ_r are normal stresses and $\tau_{r\theta}$ is the shear stress in each point of the plate thickness, with a distance equal to z from the middle surface. By integration of the stress components over the thickness of the plate, one can find the resultant forces and moments in terms of the stress components as follows:

$$\begin{aligned} (N_r, N_\theta) &= \int_{-\frac{h}{2}}^{\frac{h}{2}} (\sigma_r, \sigma_\theta) dz \\ (M_r, M_\theta) &= \int_{-\frac{h}{2}}^{\frac{h}{2}} (\sigma_r, \sigma_\theta) z dz \end{aligned} \quad (9)$$

Substituting equation (8) into equation (9), the relationship between the forces and the moments in terms of the strain components, can be calculated as:

$$\begin{aligned} \begin{pmatrix} N_r \\ N_\theta \end{pmatrix} &= A \begin{bmatrix} 1 & \nu \\ \nu & 1 \end{bmatrix} \begin{pmatrix} \varepsilon_{r0} \\ \varepsilon_{\theta0} \end{pmatrix} \\ \begin{pmatrix} M_r \\ M_\theta \end{pmatrix} &= B \begin{bmatrix} 1 & \nu \\ \nu & 1 \end{bmatrix} \begin{pmatrix} k_r \\ k_\theta \end{pmatrix} \end{aligned} \quad (10)$$

Also, by substitution of equations (6) and (7) into equations (10), the relationship between the forces and the moments in terms of the displacement components, is given by:

$$\begin{aligned}
 N_r &= A \left(\frac{du}{dr} + \frac{1}{2} \left(\frac{dw}{dr} \right)^2 + \nu \frac{u}{r} \right) \\
 N_\theta &= A \left(\frac{u}{r} + \nu \left(\frac{du}{dr} + \frac{1}{2} \left(\frac{dw}{dr} \right)^2 \right) \right) \\
 M_r &= B \left(-\frac{d^2w}{dr^2} - \frac{\nu}{r} \frac{dw}{dr} \right) \\
 M_\theta &= B \left(-\frac{1}{r} \frac{dw}{dr} - \nu \frac{d^2w}{dr^2} \right)
 \end{aligned} \tag{11}$$

The coefficients A and B are achieved by integrating the properties through the thickness of the plate as:

$$(A, B) = \int_{-\frac{h}{2}}^{\frac{h}{2}} (1, z^2) \frac{E(z)}{1-\nu^2} dz \tag{12}$$

Equilibrium equations for the circular plates can be derived by minimizing the total potential energy, or directly writing the equilibrium equations for one element. Due to axisymmetry, there are no variations along the circumference, and only the derivatives with respect to the radial direction are present in the differential equations set.

$$\begin{aligned}
 \frac{dN_r}{dr} + \frac{N_r - N_\theta}{r} &= 0 \\
 -\frac{1}{r} \frac{d}{dr} \left(r N_r \frac{dw}{dr} \right) - \frac{d^2 M_r}{dr^2} - \frac{2}{r} \frac{dM_r}{dr} + \frac{1}{r} \frac{dM_\theta}{dr} &= 0
 \end{aligned} \tag{13}$$

In order to find the stability equations from the non-linear equilibrium equations, usually the adjacent equilibrium criterion is used [5]. This criterion is used to investigate the stability and analyze the buckling behavior of the structures, based on the definition of the first and second equilibrium paths and the bifurcation point. By making use of this method one can obtain the bifurcation point, through solving the linear differential equations. It is in this manner that for an equilibrium state on the first equilibrium path, the possibility of the existence of an adjacent equilibrium form, under the same loading is investigated. Such an equilibrium form at the adjacency of the first equilibrium is the sign of the existence of a bifurcation point on the equilibrium path. The intersection point of these paths is called the bifurcation point, and at such points the equilibrium equations have two solutions, each of which corresponds to one of the two branches.

The equations necessary for this method are derived from the non-linear equilibrium equations of the structure, using the perturbation method, wherein the displacement fields (u, w) are replaced by $(u_0 + u_1, w_0 + w_1)$, in which (u_0, w_0) shows the first equilibrium state, i.e. the prebuckling state, and also indicates an equilibrium

state on the first path, and (u_1, w_1) are the infinitesimal displacements in the displacement field. But, attention should be paid to the fact that in the prebuckling state, the plate is not buckled and, or there is no lateral deflection and w_0 is equal to zero.

Substituting these new fields into the equations (13), all the terms which exclude the infinitesimal displacements are dropped out from the resulted equations. Also, if the increase in the displacement is adequately small, only the first order terms of the displacement (u_1, w_1) remain in the equations, and the higher order terms are dropped out. Therefore, the resulting stability equations are linear and homogenous equations in terms of the supposed small displacements. This recipe is recognized to be used in the determination of the stability, which is called the adjacent equilibrium criterion. Therefore, the stability equations are expressed as follows:

$$\begin{aligned} \frac{dN_{r1}}{dr} + \frac{N_{r1} - N_{\theta1}}{r} &= 0 \\ -\frac{1}{r} \frac{d}{dr} (rN_{r0} \frac{dw_1}{dr}) - \frac{d^2 M_{r1}}{dr^2} - \frac{2}{r} \frac{dM_{r1}}{dr} + \frac{1}{r} \frac{dM_{\theta1}}{dr} &= 0 \end{aligned} \tag{14}$$

Where, in the above equations:

$$\begin{aligned} N_{r1} &= A \left(\frac{du_1}{dr} + \nu \frac{u_1}{r} \right) \\ N_{\theta1} &= A \left(\frac{u_1}{r} + \nu \frac{du_1}{dr} \right) \\ M_{r1} &= B \left(-\frac{d^2 w_1}{dr^2} - \frac{\nu}{r} \frac{dw_1}{dr} \right) \\ M_{\theta1} &= B \left(-\frac{1}{r} \frac{dw_1}{dr} - \nu \frac{d^2 w_1}{dr^2} \right) \end{aligned} \tag{15}$$

$$\begin{aligned} N_{r0} &= A \left(\frac{du_0}{dr} + \nu \frac{u_0}{r} \right) \\ N_{\theta0} &= A \left(\frac{u_0}{r} + \nu \frac{du_0}{dr} \right) \\ M_{r0} &= B \left(-\frac{d^2 w_0}{dr^2} - \frac{\nu}{r} \frac{dw_0}{dr} \right) = 0 \\ M_{\theta0} &= B \left(-\frac{1}{r} \frac{dw_0}{dr} - \nu \frac{d^2 w_0}{dr^2} \right) = 0 \end{aligned} \tag{16}$$

Substitution of equations (15) and into equations (14) furnishes the stability equations in terms of the displacement components:

$$\begin{aligned} A \left(\frac{d^2 u_1}{dr^2} + \frac{1}{r} \frac{du_1}{dr} - \frac{u_1}{r^2} \right) &= 0 \\ B \nabla^4 w_1 - \frac{1}{r} \frac{d}{dr} (rN_{r0} \frac{dw_1}{dr}) &= 0 \end{aligned} \tag{17}$$

It is seen that the stability equations derived are independent from each other. Therefore, in order to determine the critical buckling pressure, the second equation has been used. In the stability equations, N_{r0} is the radial prebuckling force, which is determined from the solution of the non-linear equilibrium equations. So as to this, by substitution of equations (16) into the first relation of equation (13) we have:

$$\frac{d^2 u_0}{dr^2} + \frac{1}{r} \frac{du_0}{dr} - \frac{u_0}{r^2} = 0 \quad (18)$$

Equation (18) is called the membrane equation of plate. This equation is an ordinary linear differential equation, using whose solution one can determine the displacements and the in-plane prebuckling loads. The independent variable of this equation is u_0 , which by knowing whose value, the in-plane loads area calculated. The solution of equation (18) is as follows:

$$u_0 = c_1 r + \frac{c_2}{r} \quad (19)$$

The mechanical loading is provided by means of the application of a uniform radial load of P in Newton per meter on the edge of the plate, and in this state the edge has the ability to move freely along the radius direction. Also, due to the symmetry, the displacement at the center must be limited. As a result, the boundary conditions for the equation (19) are stated as follows:

$$\text{(At center) } \quad \text{Finite } u_0(0) = \quad (20)$$

$$N_{r0}(a) = -P \quad \text{(At edge)}$$

By applying the first boundary condition of (20) into relation (19), we have $c_2 = 0$, and by applying the second boundary condition, we have $c_1 = \frac{-P}{A(1+\nu)}$.

Therefore, relation (19) will be as follows:

$$u_0 = \frac{-rP}{A(1+\nu)} \quad (21)$$

Substitution of equation (21) into equations (16) the prebuckling forces are derived as:

$$N_{r0} = N_{\theta 0} = -P \quad (22)$$

Substitution of equation (22) into the second stability equation yields:

$$B \nabla^4 w_1 = -\frac{1}{r} \frac{d}{dr} \left(rP \frac{dw_1}{dr} \right) \quad (23)$$

By one time integration of the above relation with respect to r we have:

$$r^2 \alpha'' + r \alpha' + \alpha(\beta^2 r^2 - 1) = 0 \quad (24)$$

Where in the above:

$$\alpha = -\frac{dw_1}{dr}, \quad \beta^2 = \frac{P}{B} \tag{25}$$

Now, a new variable is defined:

$$s = \beta.r \tag{26}$$

Using which, the equation (24) becomes so:

$$s^2 \frac{d^2 \alpha}{ds^2} + s \frac{d \alpha}{ds} + (s^2 - 1)\alpha = 0 \tag{27}$$

The general answer of this equation is as follows:

$$\alpha = c_5 J_1(s) + c_6 Y_1(s) \tag{28}$$

Where J_1 and Y_1 are the Bessel type one and two functions, and C_5 and C_6 are the integration constants. At the center of the plate there is $r = s = 0$, and α must go to zero, so as to satisfy the symmetry conditions. Because s goes to zero, the $Y_1(s)$ function becomes infinity, and the above condition makes it necessary that $c_6 = 0$. In order to satisfy the clamped boundary conditions for the edges of the plate, there should be:

$$(\alpha)_{r=a} = 0 \tag{29}$$

And, therefore:

$$J_1(\beta a) = 0 \tag{30}$$

The smallest root of equation (30) is:

$$\beta a = 3.8317 \tag{31}$$

By substitution of this value into equation (25), the critical buckling pressure becomes:

$$P_{cr} = \beta^2 B = 14.6819 \frac{B}{a^2} \tag{32}$$

The answer of relation (28) can also be used for the buckling state of a circular plate, under simply supported boundary conditions. Like the clamped boundary conditions, in order to satisfy the condition existing at the center of the plate, we must have C_6 set to zero. The second condition for the simply supported boundary conditions

at $r = a$ is $M_{r1} = B \left[\frac{d\alpha}{dr} + \frac{\nu}{r} \alpha \right] = 0$. Therefore:

$$\left[\frac{dJ_1(s)}{dr} + \nu \frac{J_1(s)}{r} \right]_{r=a} = 0 \tag{33}$$

Or

$$\left[s \frac{dJ_1(s)}{ds} + \nu J_1(s) \right]_{s=\alpha a} = 0 \quad (34)$$

On the other hand, using the differentiation formulation for the Bessel functions:

$$\frac{dJ_1}{ds} = J_0 - \frac{J_1}{s} \quad (35)$$

Where J_0 is the type one Bessel function and is of order zero. Therefore:

$$\lambda a J_0(\beta a) - (1 - \nu) J_1(\beta a) = 0 \quad (36)$$

Equation (36) has different answers for different values of the Poisson's ratio, which in table (1) the smallest root has been stated for different values of ν . For example, if the Poisson's ratio is $\nu = 0.3$, according to table (1) the smallest value of βa which satisfies equation (37), is $\beta a = 2.0489$. Substituting this value into equation (25), the critical buckling pressure for the simply supported state is as follows:

$$P_{cr} = 4.1978 \frac{B}{a^2} \quad (36)$$

Table1. Smallest root of equation (36) for different values of Poisson's ratio.

	Poisson's ratio					
	0	0.1	0.2	0.3	0.4	0.5
$(\beta a)_{\min}$	1.4812	1.9154	1.9844	2.0489	2.1092	2.1659

Discussion and numerical results

In this section, the results of the exact solution of the mechanical buckling of FGM bimorph circular plates has been compared with the results of the simply supported and clamped boundary conditions, under uniform radial compression. The FGM is considered to be a compound of Aluminum as metal and Alumina as ceramic. The mechanical properties for Aluminum and Alumina have been included in table (2).

Table 2. Properties of Aluminum and Alumina, as compound elements of the FGM.

Young's (GPa) modulus	Material
70	Aluminum
380	Alumina

In tables (3) and (4) the relations used for determining the critical buckling pressure for the FGM bimorph, under clamped and simply supported boundary conditions have been stated.

Table 3. Relations for determination of the critical buckling pressure for the FGM bimorph under clamped boundary conditions.

Type of loading	Clamped
Uniform radial compression	$P_{cr} = 14.6819 \frac{B}{a^2}$

Table 4. Relations for determination of the critical buckling pressure for the FGM bimorph, under simply supported boundary conditions.

Poisson's ratio	Simply supported
0	$P_{cr} = 3.39 \frac{B}{a^2}$
0.1	$P_{cr} = 3.6687 \frac{B}{a^2}$
0.2	$P_{cr} = 3.9379 \frac{B}{a^2}$
0.3	$P_{cr} = 4.1978 \frac{B}{a^2}$
0.4	$P_{cr} = 4.4487 \frac{B}{a^2}$
0.5	$P_{cr} = 4.6911 \frac{B}{a^2}$

In order to determine the accuracy of the results achieved from solution of the stability equations for the circular plate, under clamped and simply supported boundary conditions, first the constant of the power law is set to zero, so that the FGM is turned into a homogenous material, and the dimensionless mechanical parameter λ is calculated, and the results obtained are compared with those of the other references.

By comparison with the results of the previous researches, it is observed that in the mechanical loading the dimensionless parameter of buckling λ is determined from the relation (38). In this regard, ν , D , E_c , and P_{cr} are Poisson's ratio, bending stiffness, modulus of elasticity of the ceramic, and critical radial compression loading applied on the edge in terms of Newton per meter.

$$\lambda = \frac{P_{cr} a^2}{D} \quad (38)$$

$$D = \frac{E_c h^3}{12(1-\nu^2)} \quad (39)$$

In table (5), the dimensionless parameter of mechanical buckling for the homogenous circular plate ($n=0$) with clamped and simply supported boundary conditions, and the Poisson's ratio of 0.3 has been achieved for uniform radial compression, and the results have been compared with those of the other references.

Table 5. Dimensionless Parameter of buckling for homogenous circular plate ($n=0$), under clamped and simply supported boundary conditions, with the Poisson's ratio of 0.3

Reference		h/a				
		0.001	0.01	0.05	0.1	0.2
C.a	Present	14.681 9	14.6819	14.681 9	14.681 9	14.6819
	[11]	14.68	14.68	14.68	14.68	14.68
	[4]	14.684 2	14.6842	14.684 2	14.684 2	14.6842
S.S. b	Present	4.1978	4.1978	4.1978	4.1978	4.1978
	[11]	4.2	4.2	4.2	4.2	4.2
	[4]	4.2025	4.2025	4.2025	4.2025	4.2025

a C. refers to clamped edge.
b S.S. refers to simply supported edge.

In table (6), the dimensionless parameter of mechanical buckling for the homogenous circular plate with clamped and simply supported boundary conditions, under uniform radial compression and different values of Poisson's ratio has been achieved, and the results have been compared with those of the other references. In the results, it is seen that the increase of the Poisson's ratio increases the buckling parameter.

Table 6. Dimensionless parameter of mechanical buckling for homogenous circular plate, under simply supported boundary conditions, and different Poisson's ratios.

References	Poisson's ratio					
	0	0.1	0.2	0.3	0.4	0.5
Present	3.39	3.6687	3.9379	4.1978	4.4487	4.6911
[20]	3.39	3.6687	3.9379	4.1978	4.4487	4.6911
[15]	3.389	3.668	3.937	4.199	4.448	-

After verification of the results of stability equations, the investigation of the effects of different factors on the critical buckling pressure for the FGM bimorph is performed.

Figures (2) and (3) show variations of the critical buckling pressure P_{cr} of the FGM bimorph in terms of the thickness to radius ratio of the plate, for different values of the volume fraction index, under clamped and simply supported boundary conditions, with the Poisson's ratio of 0.3. Considering the results, it is seen that the increase of h/a increases the buckling parameter for the FGM bimorphs, and the reason is that as the plate gets thicker, its stiffness increases and as a result its critical buckling compression increases, too.

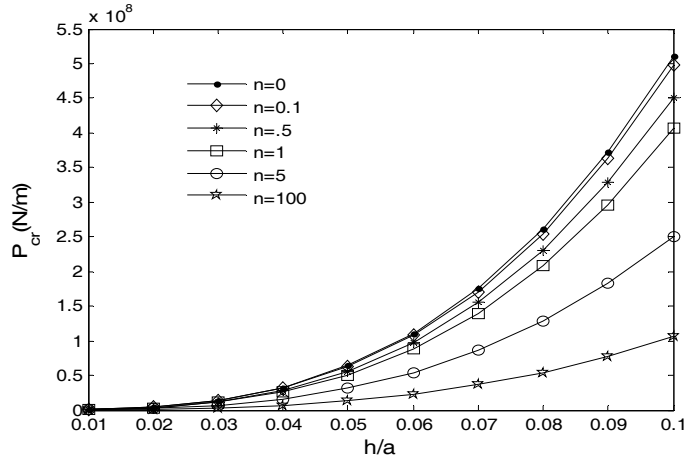


Figure 2. Variations of critical buckling pressure with respect to h/a ratio, for different values of n under clamped boundary conditions, with $\nu = 0.3$.

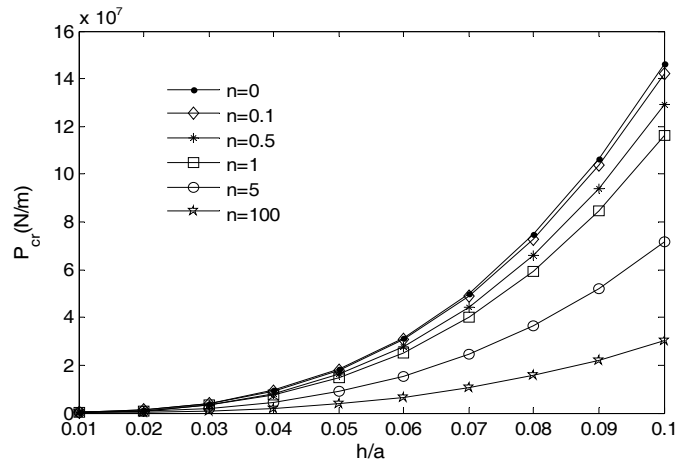


Figure 3. Variations of critical buckling pressure with respect to h/a , for different values of n under simply supported boundary conditions, with $\nu = 0.3$.

Figures (4) and (5) show the variations of the critical buckling pressure P_{cr} of the FGM bimorph with respect to the volume fraction index, for different values of the thickness to radius ratio of the plate, under clamped and simply supported boundary conditions, with the Poisson's ratio of 0.3, respectively. By the increase of the volume fraction index, the critical buckling pressure is continuously decreases, and in $n = 0$ (pure ceramic) will have its maximum value. The reason for this is that the increase of the volume fraction causes the increase of the metal volume fraction in the plate, and as the stiffness of ceramic is more than that of metal, the total stiffness of the plate is reduced, and therefore the buckling strength of the plate is reduced.

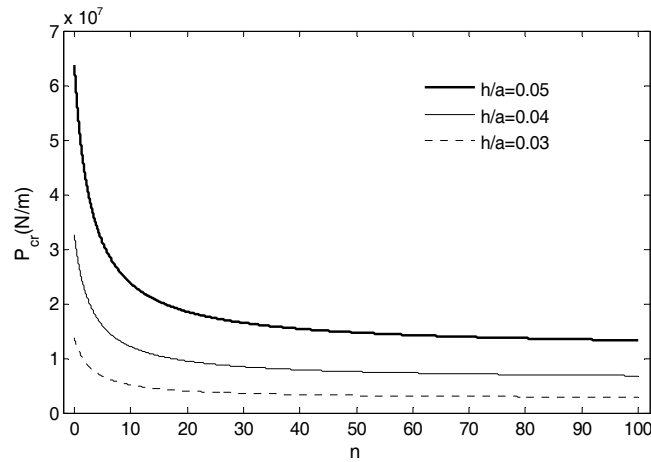


Figure 4. Variations of the critical buckling pressure with respect to n for different values of h/a under clamped boundary conditions, with $\nu = 0.3$

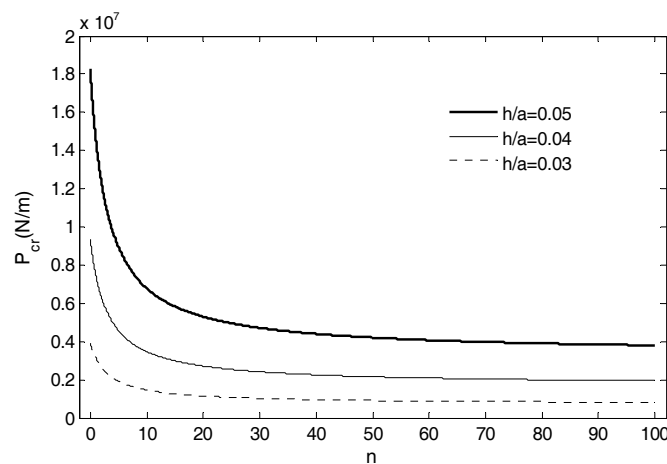


Figure 5. Variations of critical buckling temperature with respect to n , for different values of h/a , under simply supported boundary conditions, with $\nu = 0.3$

Figures (6) and (7) show variations of the critical buckling pressure with respect to the thickness to radius ratio of the plate, for different values of volume fraction index, under clamped and simply supported boundary conditions, with the Poisson's ratio of 0.3, for the two materials of one-sided FGM (reference 11) and FGM bimorph (present model). It is observed in the results that the mechanical buckling strength of the FGMs bimorphs is more than one-sided FGMs, and this difference becomes more evident in thicker plates.

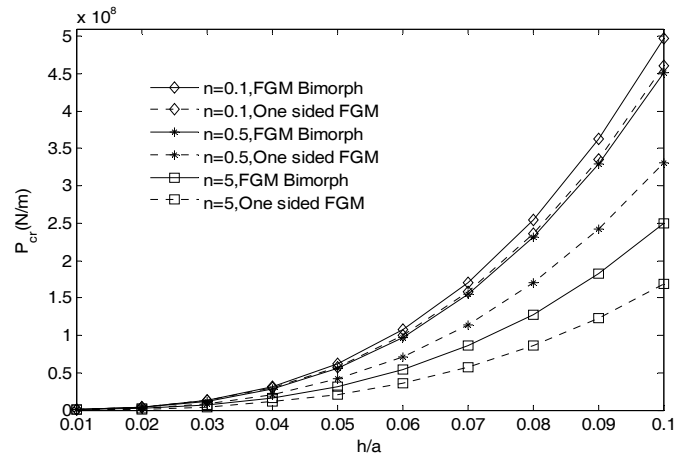


Figure 6. Variations of the critical buckling pressure with respect to h/a for different values of n under clamped boundary conditions, with $\nu = 0.3$ for two FGMs.

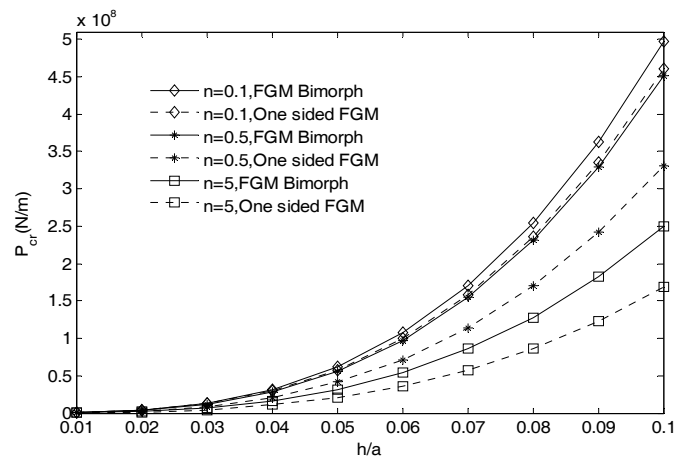


Figure 7. Variations of the critical buckling pressure with respect to h/a for different values of n under simply supported boundary conditions, with $\nu = 0.3$ for two FGMs.

Figures (8) and (9) show variations of the critical buckling pressure with respect to the volume fraction index, for different values of thickness to radius ratio of the plate, under clamped and simply supported boundary conditions, with the Poisson's ratio of 0.3, for the two materials of one-sided FGMs (reference 11) and FGM bimorphs. In the one-sided FGMs and FGM bimorphs, under clamped and simply supported boundary conditions, the critical buckling pressure continuously decreases by the increase of the volume fraction index.

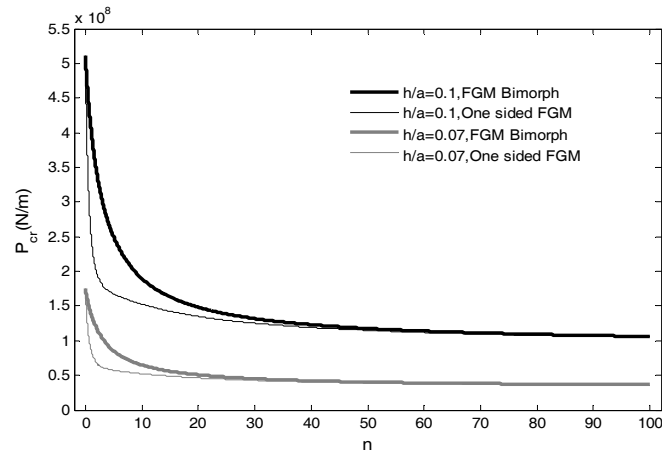


Figure 8. Variations of the critical buckling pressure with respect to n for different values of h/a under clamped boundary conditions, with $\nu = 0.3$ for two FGMs.

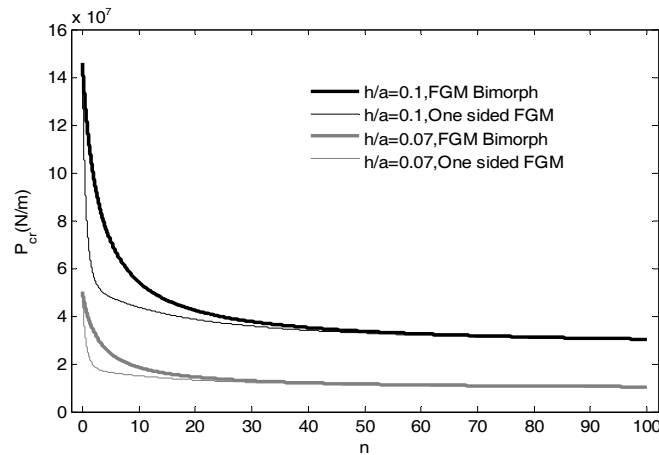


Figure 9. Variations of the critical buckling pressure with respect to n for different values of h/a under simply supported boundary conditions, with $\nu = 0.3$ for two FGMs.

Figures (10) and (11) show variations of the critical buckling pressure with respect to the thickness to radius ratio of 1, for different values of the volume fraction index and Poisson's ratio, under clamped and simply supported boundary conditions for the FGM bimorphs. It is observed in the results that in FGM bimorph circular plates, under simply supported and clamped boundary conditions, as the Poisson's ratio increases, the critical buckling strength increases. Figures (12) and (13) present the variations of the critical buckling pressure for $h/a = 0.1$, and different values of the volume fraction index and Poisson's ratio, under clamped and simply supported boundary conditions for the FGM bimorphs. It is observed in the results that in FGM

bimorphs, the critical buckling strength, under clamped boundary conditions is more than three times that of simply supported boundary conditions. The above result is also observed for homogenous materials [4].

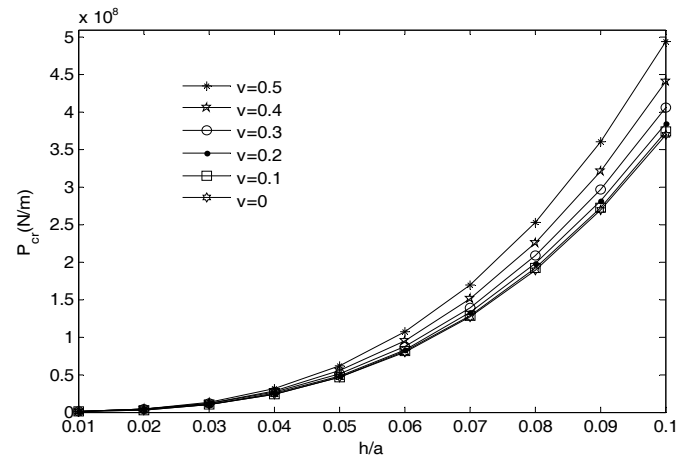


Figure 10. Variations of the critical buckling pressure for different values of h/a , and ν and $n=1$ under clamped boundary conditions.

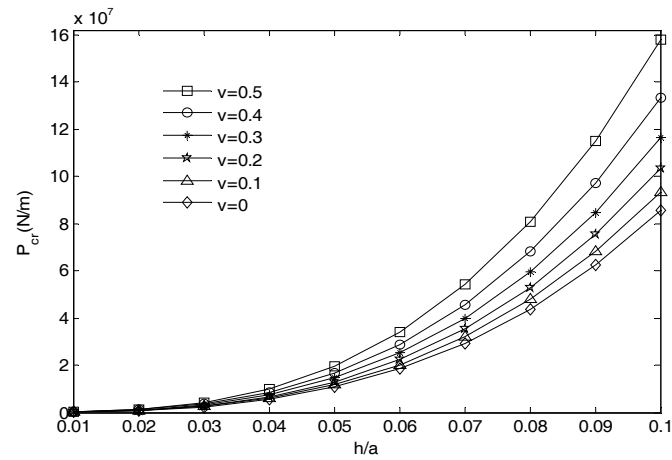


Figure 11. Variations of the critical buckling pressure for different values of h/a , and ν and $n=1$ under simply supported boundary conditions.

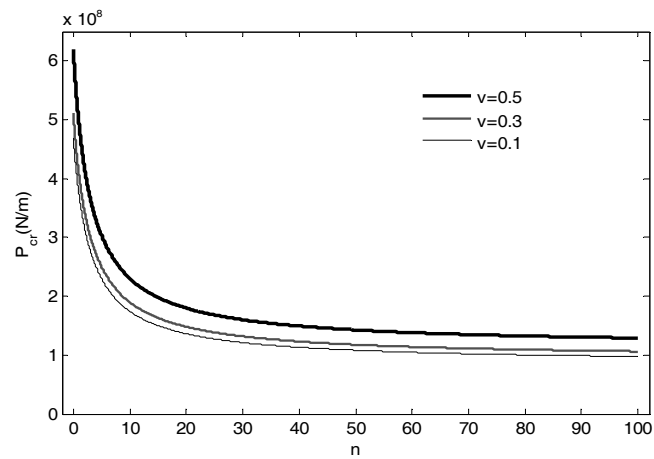


Figure 12. Variations of the critical buckling pressure for different values of n , and v and $h/a = 0.1$ under clamped boundary conditions.

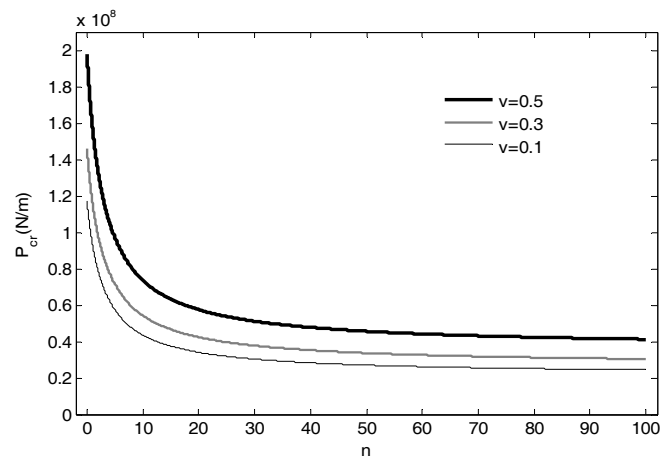


Figure 13. Variations of the critical buckling pressure for different values of n and v , and $h/a = 0.1$ under simply supported boundary conditions.

Conclusion

In the current study, the equilibrium equations have been analytically solved, and a closed-form solution is presented for the determination of the critical buckling pressure in the FGM bimorph circular plates, and the results achieved are stated as follows:

Critical buckling pressure in FGM bimorph circular plates, under simply supported and clamped boundary conditions, increases by the increase of the thickness to radius ratio of the plate.

Critical buckling pressure in FGM bimorph circular plates, under simply supported and clamped boundary conditions, decreases continuously by the increase of the volume fraction index of the plate.

Critical buckling pressure in FGM bimorph circular plates, under simply supported and clamped boundary conditions, increases by the increase of the Poisson's ratio of the plate.

Mechanical buckling strength in FGM bimorphs is higher than one-sided FGMs.

Mechanical buckling strength of the FGM bimorphs, under clamped boundary conditions is more than three times that of the simply supported boundary conditions.

References

- [1] M. Koizumi, *Ceram. Trans. Functionally Gradient Materials* (1993) 3-10.
- [2] G.H. Brayan, In: *Proceeding of the London Mathematical Society*, Vol. 22, 1891, pp. 54.
- [3] N. Yamaki, *J. Appl. Mech.* 25 (1958) 267-273.
- [4] S.P. Timoshenko, J.M. Gere, "Theory of elastic stability", New York, McGraw-Hill, 1961.
- [5] D.O. Brush, B.O. Almroth, "Buckling of bars, plates and shells", McGraw-Hill, New York, 1975.
- [6] J.N. Reddy, A.A. Khdeir, *AIAA Journal* 27 (12) (1989) 1808-1817.
- [7] K.K. Raju, G.V. Rao, *Comput. Struct.* 21 (5) (1985) 969-972.
- [8] K. K. Raju, G. V. Rao, *Comput. Struct.* 58 (3) (1996) 655-658.
- [9] M. Ozakca, N. Taysi, F. Kolcu, *Eng. Struct.* 25 (2003) 181-192.
- [10] M.M. Najafizadeh, M.R. Eslami, *AIAA Journal* 40 (7) (2002). 1444-1450.
- [11] M.M. Najafizadeh, M.R. Eslami, *Int. J. Mech. Sci.* 44 (2002) 2479-2493.
- [12] M.M. Najafizadeh, B. Hedayati, *J. Therm. Stresses* 27 (2004) 857-80.
- [13] M.M. Najafizadeh, H.R. Heydari, *Eur. J. Mech. A. Solids* 23 (2004) 1085-1100.
- [14] M.M. Najafizadeh, H.R. Heydari, *Int. J. Mech. Sci.* 50 (2008) 603-612.
- [15] M.H. Naei, A. Masoumi and A. Shamekhi, *J. Mech. Eng. Sci.* 221 (2007). 1241-1247.
- [16] S.K. Jalali, M.H. Naei, A. Poorsolhjoui, *Mater. Design* 31 (2010) 4755-4763.
- [17] Shi-Rong Li, Jing-Hua Zhang, Yong-Gang Zhao, *Thin Walled Struct.* 45 (2007) 528-536.
- [18] Chi Shyang-Ho, Chung Yen-Ling, *Int. J. Solids Struct.* 43 (2006) 3657-3674.
- [19] Ugural, A.C, "Stresses in plates and shells", WCB/McGraw-Hill edition, in English-2 nd ed, 1998.
- [20] R.Q. Xu, Y. Wang, W.Q. Chen, *Comput. Struct.* 74 (2005) 692-703.